Electrical Power and Energy Systems 75 (2016) 194–204

Contents lists available at ScienceDirect

Electrical Power and Energy Systems

journal homepage: www.elsevier.com/locate/ijepes

A two-point estimate method for uncertainty modeling in multi-objective optimal reactive power dispatch problem

Seyed Masoud Mohseni-Bonab [a], Abbas Rabiee [a,*], Behnam Mohammadi-Ivatloo [b], Saeid Jalilzadeh [a], Sayyad Nojavan [b]

[a] Department of Electrical Engineering, Faculty of Engineering, University of Zanjan, Zanjan, Iran
[b] Faculty of Electrical and Computer Engineering, University of Tabriz, Tabriz, Iran

ARTICLE INFO

Article history:
Received 20 October 2014
Received in revised form 8 August 2015
Accepted 21 August 2015

Keywords:
Monte Carlo simulation (MCS)
Multi objective optimal reactive power dispatch (MO-ORPD)
Real power loss (PL)
Two-point estimate method (TPEM)
Uncertainty
Voltage deviation (VD)

ABSTRACT

Due to nonlinear and discrete variables and constraints, optimal reactive power dispatch (ORPD) is a complex optimization problem in power systems. In this paper, the purpose is to solve multi objective ORPD (MO-ORPD) problem considering bus voltage limits, the limits of branches power flow, generators voltages, transformers tap changers and the amount of compensation on weak buses. The objectives of this paper are real power losses and voltage deviations from their corresponding nominal values, which are conflicting objectives. Because of the stochastic behavior of loads, the MO-ORPD problem requires a probabilistic approach. Hence, in this paper, a two-point estimate method (TPEM) is proposed to model the load uncertainty in MO-ORPD problem. Moreover, the proposed method is compared with some other methods such as deterministic approaches and Monte Carlo simulations (MCS). The obtained results approve the efficiency of the proposed methodology. The proposed models are implemented and solved using GAMS optimization package and verified using IEEE 14-bus and IEEE 30-bus standard test systems.

Introduction

Optimal power flow (OPF) is one of the main problems in power system operation, which was introduced by Carpentier for first time about 50 years ago [1]. Generally this problem categorized into two sub-problems, namely optimal reactive power dispatch (ORPD) and optimal real power dispatch [2]. ORPD is important for security and economy of power systems. The ORPD determines the optimal amount of reactive power generation at different places, which is used for minimization of real power transmission losses and total voltage deviation with considering different equality and inequality constraints. Nonlinear objective function and different type of constraints makes the ORPD problem a large-scale nonlinear optimization problem.

The ORPD problem is modeled for different objective functions and various methods are used for its solution. As presented in [3], the reactive power generation management can be employed to improve the voltage stability margin of power systems. A solution to the reactive power dispatch problem with a particle swarm optimization approach based on multi-agent systems is presented in [4]. In [5], a model for ORPD is presented for minimization of the total costs. The total cost is defined as cost of energy loss of transmission network and the costs of adjusting the control devices. In [6], a harmony search algorithm is implemented for solution of ORPD problem. In this paper, different objective functions including power transmission loss, voltage stability and voltage profile are optimized separately. Hybrid methods are also used for solution of ORPD problem to provide the advantage of different methods simultaneously. Hybridization of modified teaching learning algorithm and double differential evolution algorithm has been used in [7] for effective solution of ORPD problem. In [8], hybrid standard real-coded genetic algorithm and simulated annealing method is used to solve ORPD problem. In [9], application of chance-constrained programming method to handle the uncertainties in ORPD problem is studied. Uncertain nodal power injections and random branch outages are considered as uncertainty sources. The problem is solved by combining probabilistic power flow and genetic algorithm. The differential evolution algorithm for optimal settings of reactive power dispatch control variables is employed in [10].

ORPD problem is modeled as multi-objective optimization problem and solved using different methods in literature. A

* Corresponding author at: Department of Electrical Engineering, Faculty of Engineering, University of Zanjan, P.O. Box: 45371-38111, Zanjan, Iran. Tel.: +98 2433054208; fax: +98 2433052762.

E-mail addresses: s.m.mohsenibonab@ieee.org (S.M. Mohseni-Bonab), rabiee@znu.ac.ir (A. Rabiee), mohammadi@ieee.org (B. Mohammadi-Ivatloo), jalilzadeh@znu.ac.ir (S. Jalilzadeh), sayyad.nojavan@tabrizu.ac.ir (S. Nojavan).

http://dx.doi.org/10.1016/j.ijepes.2015.08.009
0142-0615/

Nomenclature

Sets
N_B/N_j set of buses
N_L set of branches (transmission lines)
N_G set of generating units
N_D set of load buses
ψ_ℓ set of buses adjacent to ℓ-th branch
N_T set of tap changing transformers
N_{sh} set of VAR compensators
N_O set of objective functions
N_P set of Pareto optimal solutions

Indices
k index of Pareto optimal solutions
i/j index of bus number where $i = 1, 2, \ldots, N_B$
ℓ index of transmission lines
sl index of slack bus
r index of objective functions
t index of on-load tap changing transformers

Parameters
w_1 weight of objective 1 (real power loss)
w_2 weight of objective 2 (voltage deviation)
$y_\ell/g_\ell/b_\ell$ Admittance/conductance/susceptance of ℓ-th line
$Y_{ij} = G_{ij} + jB_{ij}$ ij-th element of system Y_{BUS} matrix
P_{Gi} active power production at bus i
$P_{G_i}^{\min}/P_{G_i}^{\max}$ minimum/maximum value for active power
$T_t^{\min}/T_t^{\max}$ minimum/maximum value for t-th tap changer settings
P_{D_i} real power of the i-th bus
Q_{D_i} reactive power of the i-th bus
$Q_{G_i}^{\min}/Q_{G_i}^{\max}$ minimum/maximum value for reactive power of the i-th bus
$V_i^{\min}/V_i^{\max}$ minimum/maximum value for voltage magnitude of the i-th bus
$S_\ell^{\max}$ maximum value of power flow of ℓ-th transmission line
Q_{C_i} VAR compensation capacity in each step at bus i
$A_i^{\min}/A_i^{\max}$ minimum/maximum reactive power compensation step at bus i

Variables
x vector of dependent variables
u vector of control variables
T_t value of t-th tap changer setting
V_i/V_j voltage magnitude of bus i/j
θ_i/θ_j voltage angle at bus i/j
S_ℓ power flow of ℓ-th transmission line
Q_{G_i} reactive power generation in bus i
A_i reactive power compensation step at bus i
Q_{sh_i} reactive power compensation at bus i

Functions
J total objective function
J_1 first objective function (PL = real power loss)
J_2 second objective function (VD = voltage deviation)
J_{pu} normalized objective function (PL_{pu} and VD_{pu})
$J_r^{\max}/J_r^{\min}$ maximum/minimum value for r-th objective function
$PL^{\min}/PL^{\max}$ minimum/maximum value for PL
$VD^{\min}/VD^{\max}$ minimum/maximum value for VD

strength Pareto evolutionary algorithm is proposed in [11] to handle the ORPD problem considering the real power loss and the bus voltage deviations as objective functions. In [12], real power loss, voltage deviation and voltage stability index are considered as objective functions and the obtained multi-objective problem is solved using teaching learning based optimization algorithm. Improving voltage stability margin of power system [13] by controlling VAR sources is studied in [14,15]. In [15], *L-index* is used as voltage stability index and is incorporated in multi-objective ORPD problem considering active power losses as another objective. The problem is solved using chaotic PSO based multi-objective optimization method. In [16], ORPD problem is modeled as fuzzy goal programming problem and solved using genetic algorithm. ORPD problem considering static voltage stability and voltage deviation is solved using a seeker optimization algorithm (SOA) in [17]. The multi-objective ORPD problem considering active power losses and voltage stability index as objective functions is solved using modified NSGA-II in [18]. In [19], a hybrid fuzzy multi-objective evolutionary algorithm based approach is proposed for solution of multi-objective ORPD problems. Hybrid modified imperialist competitive algorithm and invasive weed optimization is implemented in [20] for multi-objective ORPD (MO-ORPD) problem solution. In [21], different constraint handling methods in ORPD problem including feasible solutions, self-adaptive penalty, ε-constraint, stochastic ranking, and the ensemble of constraint handling techniques is evaluated. A multi objective chaotic parallel vector evaluated interactive honey bee mating optimization algorithm is presented in [22] to solve the MO-ORPD problem with considering operational constraints of the generators.

Therefore, it is observed that the MO-ORPD problem has been solved so far with many intelligent algorithms but none of them solve multi objective reactive power dispatch considering load uncertainty. Load forecast can be obtained using historical load data and whether forecast data using different methods. But, always the forecast is not perfect and there is an inaccuracy in the forecasted data. Therefore it is necessary to consider the effect of uncertain loads in the problem.

Uncertain parameters in power systems can be divided into two categories: The first one is technical parameters like outages, demand and generation and second one is economical parameters like as inflation rate or price levels. There are different methodologies for handling uncertainties in power systems that is based on aforementioned parameters. Stochastic programming is widely used in power system planning and operation for uncertainty modeling [23–25]. In stochastic programming based methods, the uncertain parameters are modeled using discrete scenarios with their occurrence probability. Information gap decision theory (IGDT) is a non-possibilistic uncertainty modeling method, which does not require probability distribution of the uncertain parameters. IGDT method is used for modeling wind power generation uncertainty in OPF problem in presence of HVDC lines [26]. This method is also used for modeling price uncertainty in operation of generation companies [27] and distribution companies [28]. Robust optimization is another decision making tool in uncertain environments. This method is utilized in [29] for market price uncertainty modeling in optimal self-scheduling of a hydro-thermal generating company. In [30], robust optimization method is used for decision making of a retailer in energy market. An updated review of the uncertainty modeling methods in energy systems are provided in [31].

The aim of this paper is determining optimal values of control variables in order to achieve the objectives such as reducing real power losses and minimizing voltage deviation considering the technical constraints as well as some existing uncertainties. In order to model the load uncertainty, the Hong's two-point estimate method (TPEM) is used. The main feature of the proposed TPEM is that it only requires resolving $2 \times m$ deterministic MO-ORPD to obtain the behavior of m random variable. Since this paper focuses on the uncertainties involved by the load, it is assumed that their statistical features are estimated or measured. The main contributions of this work are summarized as follows:

(1) The stochastic behavior of load is modeled using TPEM.
(2) Similar to the Monte Carlo simulation (MCS) approaches, TPEM use the deterministic routines for solving the probabilistic MO-ORPD. However, they require a much lower computational burden.
(3) Furthermore, PEM overcome the difficulties associated with the lack of perfect knowledge of the probability functions of stochastic variables, since these functions are approximated using only their first few statistical moments (i.e., mean, variance, skewness, and kurtosis). Therefore, a smaller level of data information is needed.

The rest of the paper is organized as follows: Section 'ORPD problem formulation' and 'Multi objective optimal reactive power dispatch (MO-ORPD)' describe the reactive power dispatch problem formulation and MO-ORPD problem, respectively. Implementation of TPEM on the problem is presented in Section 'Implementation of TPEM'. Section 'Case study' describes the numerical example used in this paper. A brief summary of the simulation results, the obtained numerical results, and some other observations and discussions, are also included in this section. Finally, the contributions and conclusions of this paper are summarized in last section.

ORPD problem formulation

A system operator usually has various objectives such as minimization of sum of system transmission loss and voltage deviation of load buses from their desired values. These objective functions may conflict with each other. Hence, at the first, the confliction among them is investigated. The conventional ORPD model can be described mathematically as follows.

ORPD objective functions

In this paper the objective functions are minimization of real power losses and voltage deviation in load buses.

Minimization of total real power losses

With the increasing rate of energy consumption, the amount of power losses increased too, making the reduction of power losses as an important aim for system operators [32,33]. The active power losses can be expressed as follows.

$$J_1 = PL(x,u) = \sum_{\substack{\ell=1 \\ i,j\in\Psi_\ell}}^{N_L} g_\ell [V_i^2 + V_j^2 - 2V_iV_j\cos(\theta_i - \theta_j)] \quad (1)$$

Minimization of voltage deviation at load bus

The second objective of ORPD problem is to maintain a proper voltage level at load buses. Electrical equipment is designed for optimum operation of nominal voltage. The deviation from the nominal voltage will decrease the efficiency and life of the electrical devices. Thus, the voltage profile of the system could be optimized by minimization of the sum voltage deviations from the corresponding rated values at load buses. This objective function is defined as follows:

$$J_2 = VD(x,u) = \sum_{i=1}^{N_D} |V_i - V_i^{spc}| \quad (2)$$

Constraints

Equality constraints (AC power flow equations)

The AC power flows equations are expressed as follows.

$$\begin{aligned} P_{G_i} - P_{D_i} &= V_i \sum_{j=1}^{N_B} V_j [G_{ij}\cos(\theta_i - \theta_j) + B_{ij}\sin(\theta_i - \theta_j)] \\ Q_{G_i} - Q_{D_i} + Q_{sh_i} &= V_i \sum_{j=1}^{N_B} V_j [G_{ij}\sin(\theta_i - \theta_j) - B_{ij}\cos(\theta_i - \theta_j)] \end{aligned} \quad (3)$$

Operational limits

The generators active and reactive power outputs along with bus voltages should be hold in a pre-specified interval, as follows:

$$P_{G_i}^{\min} \leqslant P_{G_i} \leqslant P_{G_i}^{\max}, \quad \forall i = \{sl\} \quad (4)$$

$$Q_{G_i}^{\min} \leqslant Q_{G_i} \leqslant Q_{G_i}^{\max}, \quad \forall i \in N_G \quad (5)$$

$$V_i^{\min} \leqslant V_i \leqslant V_i^{\max}, \quad \forall i \in N_B \quad (6)$$

Also, the line flow limits are as follows.

$$|S_\ell| \leqslant S_\ell^{\max}, \quad \forall \ell \in N_L \quad (7)$$

Also, on-load tap changing transformers (OLTC) settings are modeled in this paper. As it is depicted in Fig. 1, the OLTC connected between buses i and j will change three elements of system Y_{BUS} corresponding to ii-th, ij-th and ji-th elements.

$$Y_{BUS} = \begin{bmatrix} \cdots & & & & \cdots \\ & & i\downarrow & j\downarrow & \\ & i\rightarrow & \frac{y_\ell}{T_t^2} & -\frac{y_\ell}{T_t} & \\ \cdots & & & & \cdots \\ & j\rightarrow & -\frac{y_\ell}{T_t} & y_\ell & \\ \cdots & & & & \cdots \end{bmatrix} \quad (8)$$

The OLTC settings should be restricted by their lower and upper limits as follows:

$$T_t^{\min} \leqslant T_t \leqslant T_t^{\max}, \quad \forall t \in N_T \quad (9)$$

It is worth to note that the reactive power output of VAR compensation devices are modeled as a multi-step compensation, i.e. a discrete variable is defined for each VAR compensation node as follows, which determine how many steps of VAR injections are necessary.

$$Q_{sh_i} = Q_{C_i} \times A_i, \quad \forall i \in N_{sh} \quad (10)$$

The reactive power compensation steps are limited as follows.

$$A_i^{\min} \leqslant A_i \leqslant A_i^{\max}, \quad \forall i \in N_{sh} \quad (11)$$

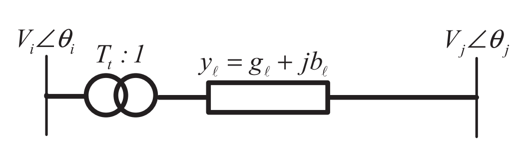

Fig. 1. OLTC model used in this paper.

Multi objective optimal reactive power dispatch (MO-ORPD)

Various methods are available to solve multi-objective optimization problems such as weighted sum approach [34], ε-constraint method [24], and evolutionary algorithms [35]. In this paper, the proposed multi-objective model of the MO-ORPD is solved using the weighted sum method.

In the weighted sum method, different weights are used for the conflicting objective functions to generate different Pareto optimal solutions and then the different weights selects the most satisfactory solution from the optimal Pareto set. In the weighted sum method, the problem is solved as follows:

$$\min[J(x,u)] = w_1 J_{1,pu}(x,u) + w_2 J_{2,pu}(x,u) \tag{12}$$

where

$$w_1 + w_2 = 1 \tag{13}$$

The aforementioned MO-ORPD problem can be formulated mathematically as a nonlinear constrained optimization problem, which can be expressed as:

$$\begin{aligned} x^T &= \left[[V_L]^T, [Q_G]^T, [S_L]^T\right] \\ u^T &= \left[[V_G]^T, [Q_C]^T, [T]^T\right] \end{aligned} \tag{14}$$

Fuzzy modeling for normalizing objective functions

Since the objective functions (1) and (2) are not in the same range and dimension, a fuzzy satisfying method is proposed to calculate the normalized form of the objective functions in (12). The fuzzy membership of each objective function maps it to the interval [0,1]. More generally, the i-th objective function of J_i is normalized as follows:

$$J_{r,pu}^{(k)} = \begin{cases} 1 & J_r^{(k)} \leqslant J_r^{\min} \\ \frac{J_r^{(k)} - J_r^{\max}}{J_r^{\min} - J_r^{\max}} & J_r^{\min} \leqslant J_r^{(k)} \leqslant J_r^{\max}, \quad \forall r = 1,\ldots,N_O, \quad \forall k = 1,\ldots,N_P \\ 0 & J_r^{(k)} \geqslant J_r^{\max} \end{cases} \tag{15}$$

For the entire Pareto optimal set, the number of best compromise solution (BCS) is obtained by using min–max criterion [36] as follows.

$$\max_k \left(\min_r (J_{r,pu}) \right) \tag{16}$$

This means that the solution which has the largest value of $\min_r(J_{r,pu})$, is the BCS. In this paper for objective functions (1) and (2), the normalized values are expressed as:

$$PL_{pu} = J_{1,pu} = \frac{PL - PL^{\max}}{PL^{\min} - PL^{\max}} \tag{17}$$

$$VD_{pu} = J_{2,pu} = \frac{VD - VD^{\max}}{VD^{\min} - VD^{\max}} \tag{18}$$

Solution tool

In this paper the stochastic multi-objective reactive power dispatch problem is formulated as a mixed integer nonlinear programming (MINLP) problem, and it is solved using Generalized Algebraic Modeling Systems (GAMS) software [37]. Also, CONOPT [38] and SBB [39] solvers are utilized for dealing with nonlinear programming (NLP) and MINLP problems, respectively.

Implementation of TPEM

Monte-Carlo simulation is an iterative approach which utilizes cumulative density function (CDF) of random variables to determine the final result. This method is widely used for uncertainty modeling. Requiring great number of iterations to reach the desired convergence is the main drawback of the MCS. The TPEM is an approximate method. The information provided by central moments is used to find some representative points (s points for each variable) named concentrations. These representative points are used for solution of the model and the statistical information of the random output variable is calculated using the solutions obtained for representative points [40].

Assume that $X\{x_1, x_2, \ldots, x_l, \ldots, x_m\}$ is a random variable with a mean value μ_{x_l} and standard deviation σ_{x_l}. Moreover, Z is a random function of X (i.e. $Z = F(X)$). Each of the s concentrations of variables x_l can be defined as a pair composed of a location $x_{l,s}$ and a weight $w_{l,s}$. The proposed method uses a particular case of point estimate method, known as Hong's two-point estimate method (HTPEM). Using HTPEM, function F has to be evaluated only s times for each random input variable x_l at the points made up of the sth location of random input variable x_l and the mean value (μ_{x_l}) of remaining input variables. Therefore, the total number of evaluations is $2 \times m$. The location $x_{l,s}$ is determined as follows [41]:

$$x_{l,s} = \mu_{x_l} + \xi_{l,s} \cdot \sigma_{x_l} \tag{19}$$

In which, $\xi_{l,s}$ is the standard location of random variable x_l. The standard locations and weights of random variable of x_l are computed by:

$$\xi_{l,1} = \frac{\lambda_{l,3}}{2} + \sqrt{m + \left(\frac{\lambda_{l,3}}{2}\right)^2}, \quad \xi_{l,2} = \frac{\lambda_{l,3}}{2} - \sqrt{m + \left(\frac{\lambda_{l,3}}{2}\right)^2} \tag{20}$$

and

$$w_{l,1} = -\frac{\xi_{l,2}}{m(\xi_{l,1} - \xi_{l,2})}, \quad w_{l,2} = \frac{\xi_{l,1}}{m(\xi_{l,1} - \xi_{l,2})} \tag{21}$$

where $\lambda_{l,3}$ denotes the skewness of the random variable x_l:

$$\lambda_{l,3} = \frac{E\left[(x_l - \mu_{x_l})^3\right]}{(\sigma_{x_l})^3} \tag{22}$$

The algorithm of solving the MO-ORPD problem by means of HTPEM is shown in Fig. 2.

In the MO-ORPD problem, the load is modeled as random variable with known probability distribution. The locations and weights have to be computed as described previously. A deterministic MO-ORPD must be run for each concentration. The solution of an MO-ORPD is:

$$Z_{l,s} = F\{x_{l,1}, x_{l,2}, \ldots, x_{l,s}, \ldots, x_{m,s}\} \tag{23}$$

where $Z_{l,s}$, is the vector of random output variables associated with the sth concentration of random input variable and represents the nonlinear relation between the input and output variables in the MO-ORPD. The raw moments of output random variables are determined as:

$$E(Z) \cong E(Z) + \sum_s w_{l,s} \cdot Z_{l,s} \tag{24}$$

To clarify the flowchart of algorithm, the solution steps are summarized as follows:

Step 1: Set the first and second moments of sth output random variables to zero: $E(Z) = 0$.
Step 2: Select the input random variable x_l.
Step 3: Compute $\lambda_{l,3}, \xi_{l,s}, w_{l,s}$ based on (19)–(22).

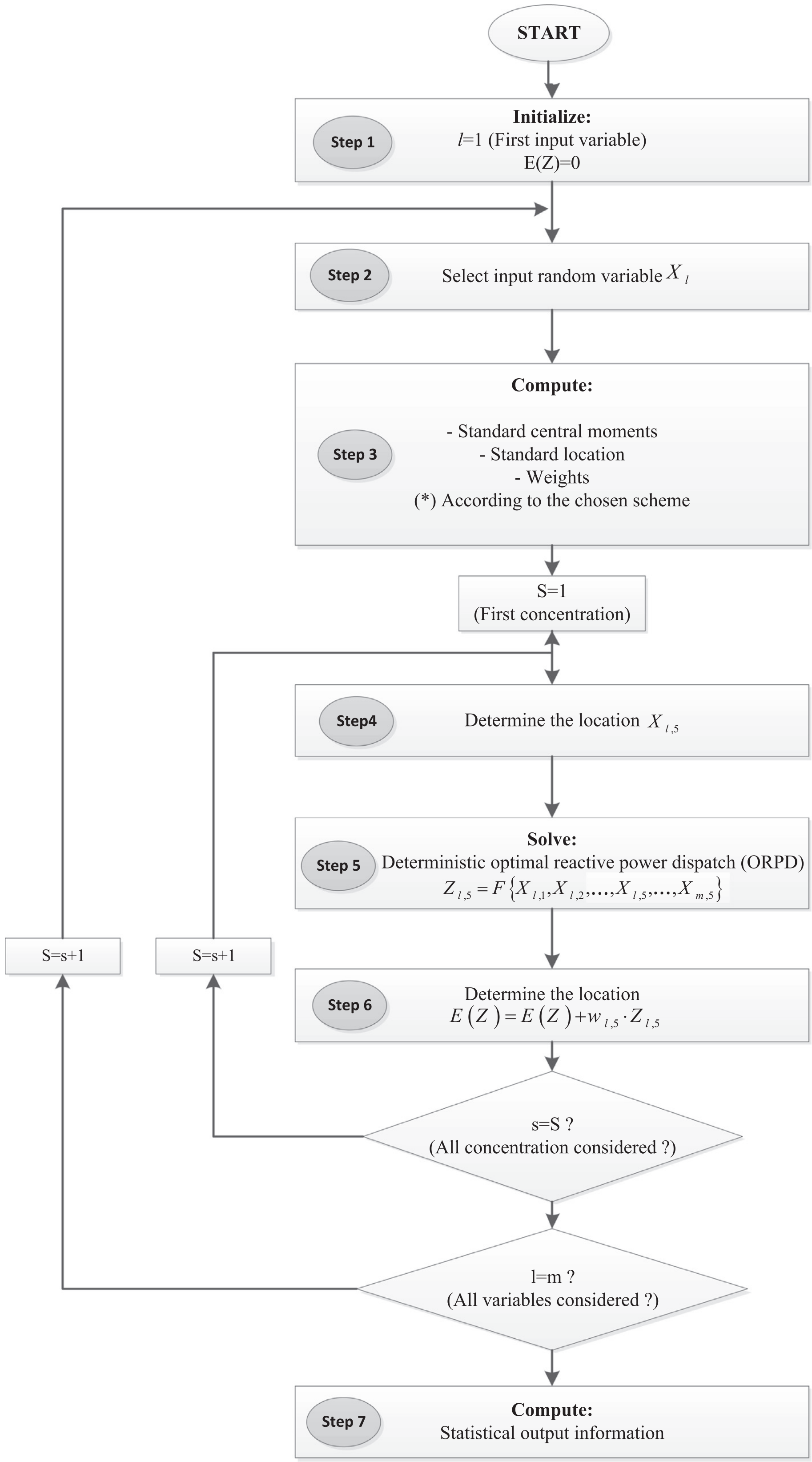

Fig. 2. Flowchart of the proposed algorithm.

Step 4: Determine the two estimated locations of $x_{l,s}$.
Step 5: Solve the deterministic MO-ORPD for each concentration.
Step 6: Update the raw moments of output variables.

Step 7: Repeat the steps 2–6 until all concentrations of all input random variables are taken into account. Finally, compute the statistical information of output random variables.

Case study

Test systems

Simulation is carried out on IEEE 14-bus and IEEE 30-bus standard test systems.

Case I: IEEE 14-bus system [10,42] consists of 14 buses, which 5 of them are generator buses. Bus 1 is the slack bus, 2, 3, 6 and 8 are taken as PV buses and the remaining 9 buses are PQ buses. The network has 20 branches, 3 transformers and 4 capacitor banks. The three branches 4–7, 4–9, 5–6 are equipped with under load tap changing transformers which their taps is within the interval [0.9, 1.1]. Two capacitor banks are available at weak buses 9 and 14. Each capacitor bank consists of three 6 MVAr steps. The dimension of control variables is 17, which consist of five PV generator voltages within the range of [0.9, 1.1] and power output of slack bus generator in the interval [0, 323.4] MW, three tap changing transformers within the range of [0.9, 1.1] and two shunt compensation capacitor banks. The topology and initial operating conditions of this system are given in [42].

Case II: IEEE 30-bus system [42] consists of 30 buses, out of which 6 are generator buses. Bus 1 is the slack bus. The network has 41 branches, 4 transformers and 9 capacitor banks. The dimension of control variable is 25. The initial operating conditions of the system are given by [42]. According to [12], shunt capacitors are installed at buses 10, 12, 15, 17, 20, 21, 23 and 29. Also, each VAR compensation device is assumed to be 6 steps of 6 MVAR.

In order to clearly illustrate the effectiveness of proposed method, a comparison among the results of three different cases:

(I) Deterministic optimization (ignoring the uncertainty in input parameter).
(II) Uncertainty characterization using TPEM.
(III) Uncertainty characterization using MCS.

The simulation results are described as follows.

Case I: IEEE-14 bus system

Deterministic optimization

In Case I, only the mean value of load is considered in the MO-ORPD problem. Real power loss and voltage deviation are considered as objective functions simultaneously.

In order to solve the multi-objective RPD problem by weighted sum method, maximum and minimum values of the expected real power loss (i.e. f_1) and voltage deviation (i.e. f_2) are calculated, which are equal to 14.33382 MW, 13.08294 MW, 0.02925 pu and 0.00147 pu, respectively. These border values are achieved by maximizing and minimizing the objective functions of MO-ORPD individually.

Table 1 shows the values of both objective functions for all 11 Pareto optimal solutions. Among these optimal solutions, Solution#1 is the minimum power loss, with the equal to 13.08294 MW and the *VD* of 2.9% (minimum *VD*).

As explained in Section 'Fuzzy modeling for normalizing objective functions', in order to select the best solution among the obtained Pareto optimal set, a fuzzy satisfying method is utilized here. It is evident from the last column of Table 1 that the BCS is *Solution#7*, with the maximum weakest membership function of 0.82695. The corresponding MO-ORPD problem real power loss and *VD* are equal to 13.29397 MW and 0.00628 pu, respectively. Correspondingly, the Pareto optimal front of the two objective functions is derived, which is depicted in Fig. 3. This Pareto front consists of 11 Pareto optimal solutions.

Uncertainty characterization using TPEM

Due to the stochastic behavior of the load, the MO-ORPD problem analysis requires a probabilistic approach. In this section, a TPEM is employed to model the uncertainty in load with considering the mean and standard deviation values of load. In this case, the expected objective functions are higher than the deterministic case. The mean values of real power loss and voltage deviation of MO-ORPD for this case are also summarized in Table 2. According to Table 2 Solution#7 is the BCS. The Pareto optimal front of the two objective functions is derived, which is depicted in Fig. 4. This Pareto front consists of 11 Pareto optimal solutions.

Uncertainty characterization using MCS

In this section, MCS is used to deal with the aforementioned uncertainties. The MCS is a numerical simulation procedure applied to the problems involving random variables with known

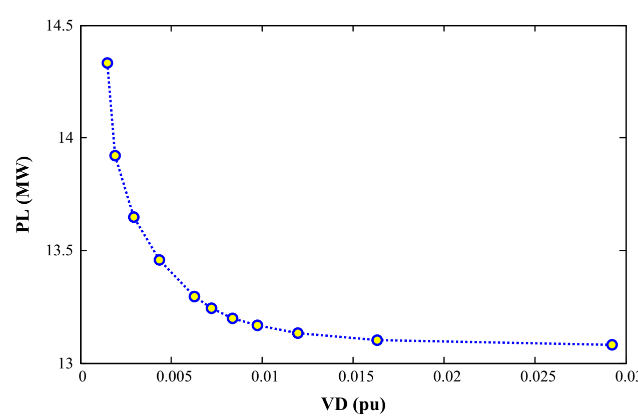

Fig. 3. Pareto front of deterministic case for IEEE 14-bus system.

Table 1
Pareto optimal solution of deterministic case for IEEE 14-bus system.

#	w_1	w_2	*PL* (MW)	*VD* (pu)	$J_{1,pu} = \frac{PL_{max}-PL}{PL_{max}-PL_{min}}$	$J_{2,pu} = \frac{VD_{max}-VD}{VD_{max}-VD_{min}}$	$\min(J_{1,pu}.J_{2,pu})$
1	1.0	0.0	13.08294	0.02925	1	0	0
2	0.9	0.1	13.10148	0.01631	0.98518	0.46584	0.46584
3	0.8	0.2	13.13466	0.01196	0.95865	0.62236	0.62236
4	0.7	0.3	13.1677	0.00972	0.93224	0.70321	0.70321
5	0.6	0.4	13.19957	0.00839	0.90676	0.75105	0.75105
6	0.5	0.5	13.24408	0.00719	0.87118	0.79415	0.79415
7	**0.4**	**0.6**	**13.29397**	**0.00628**	**0.83130**	**0.82695**	**0.82695**
8	0.3	0.7	13.45718	0.00435	0.70082	0.89629	0.70082
9	0.2	0.8	13.64897	0.00293	0.54750	0.94755	0.54750
10	0.1	0.9	13.92241	0.00190	0.32890	0.98465	0.32890
11	0.0	1.0	14.33382	0.00147	0	1	0

The bold numbers correspond to the best compromise Pareto optimal solution.

Table 2
Pareto optimal solution of TPEM for IEEE 14-bus system.

#	w_1	w_2	PL (MW)	VD (pu)	$J_{1,pu} = \frac{PL_{max}-PL}{PL_{max}-PL_{min}}$	$J_{2,pu} = \frac{VD_{max}-VD}{VD_{max}-VD_{min}}$	$\min(J_{1,pu}, J_{2,pu})$
1	1.0	0.0	13.09301	0.02856	1	0	0
2	0.9	0.1	13.11238	0.0162	0.98454	0.45635	0.45635
3	0.8	0.2	13.14655	0.01185	0.95725	0.61699	0.61699
4	0.7	0.3	13.18318	0.00947	0.928	0.70488	0.70488
5	0.6	0.4	13.21372	0.00823	0.90363	0.7506	0.7506
6	0.5	0.5	13.2563	0.00712	0.86962	0.79179	0.79179
7	**0.4**	**0.6**	**13.30514**	**0.00625**	**0.83064**	**0.82377**	**0.82377**
8	0.3	0.7	13.47842	0.00427	0.69229	0.89704	0.69229
9	0.2	0.8	13.67139	0.00288	0.53822	0.94833	0.53822
10	0.1	0.9	13.94164	0.00189	0.32245	0.98492	0.32245
11	0.0	1.0	14.3455	0.00148	0	1	0

The bold numbers correspond to the best compromise Pareto optimal solution.

or assumed probability distributions. It consists of repeating a deterministic simulation process, where in each simulation, a particular set of values for the random variables are generated according to the corresponding probability distributions. The result of MCS is similar to a sample of an experimental observation. By collecting the results of many such simulations, it is possible to apply the methods of statistical estimation and inference to the data set obtained.

For load buses, the random variable to be treated by the simulation procedure is load considering its stochastic behavior. It is assumed that this variable is normally distributed with a known mean value (corresponding to the forecasted value) and a 5% standard deviation.

The appropriate values of random variables are generally achieved by inverting the cumulative distribution function. In

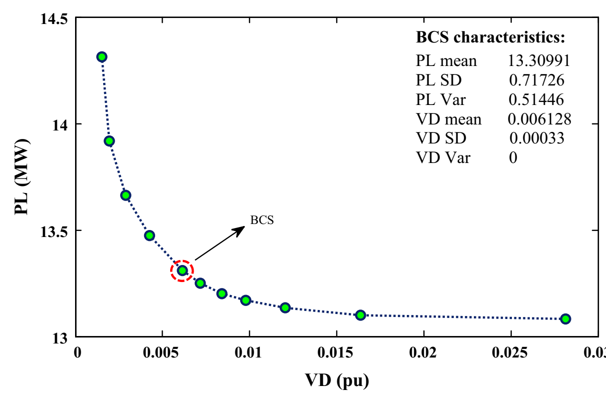

Fig. 5. Pareto front of MCS for IEEE 14-bus system.

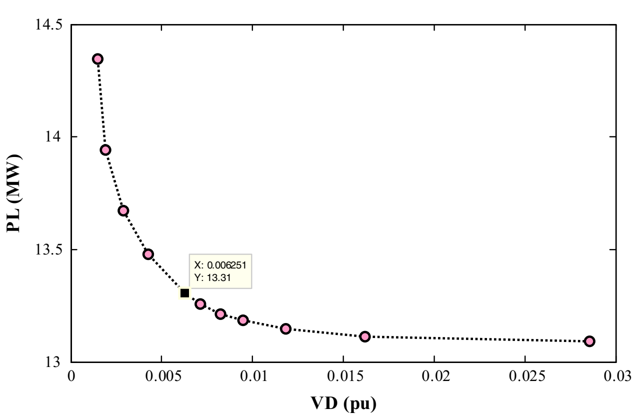

Fig. 4. Pareto front of TPEM for IEEE 14-bus system.

Table 4
Control variables for the best solution in IEEE 14-bus system.

Control variables	Deterministic approach	MCS (mean)	TPEM (mean)
Generator variables			
Vg_1 (pu)	1.06	1.05921	1.059895
Vg_2 (pu)	1.03528	1.03455	1.035015
Vg_3 (pu)	0.99919	0.99862	0.99898
Vg_6 (pu)	1.02437	1.02407	1.02404
Vg_8 (pu)	1.00945	1.0096	1.008995
Pg_1 (MW)	227.294	227.158	227.3203
Shunt compensation ($A \times Q_C$)			
Qc_9 (MVar)	0	0	0
Qc_{14} (MVar)	1×6	0.9462×6	1×6
Transformer tap changer			
T_{4-7} (pu)	0.96816	0.96732	0.96883
T_{4-9} (pu)	1.08422	1.08153	1.082185
T_{5-6} (pu)	0.98957	0.98926	0.989645

Table 3
Pareto optimal solution of MCS for IEEE 14-bus system.

#	w_1	w_2	PL (MW)	VD (pu)	$J_{1,pu} = \frac{PL_{max}-PL}{PL_{max}-PL_{min}}$	$J_{2,pu} = \frac{VD_{max}-VD}{VD_{max}-VD_{min}}$	$\min(J_{1,pu}, J_{2,pu})$
1	1.0	0.0	13.08053	0.028124	1	0	0
2	0.9	0.1	13.0999	0.016391	0.98430	0.44102	0.44102
3	0.8	0.2	13.13422	0.012028	0.95648	0.60500	0.60500
4	0.7	0.3	13.16835	0.009778	0.92881	0.68957	0.68957
5	0.6	0.4	13.20198	0.008429	0.90154	0.74028	0.74028
6	0.5	0.5	13.2492	0.007181	0.86326	0.78720	0.78720
7	**0.4**	**0.6**	**13.30991**	**0.006128**	**0.81405**	**0.82676**	**0.81405**
8	0.3	0.7	13.47235	0.004255	0.68236	0.89716	0.68236
9	0.2	0.8	13.66353	0.002876	0.52738	0.94901	0.52738
10	0.1	0.9	13.91945	0.001927	0.31991	0.98468	0.31991
11	0.0	1.0	14.31407	0.001519	0	1	0

The bold numbers correspond to the best compromise Pareto optimal solution.

Table 5
Pareto optimal solution of deterministic case for IEEE 30-bus system.

#	w_1	w_2	*PL* (MW)	*VD* (pu)	$J_{1,pu} = \frac{PL_{max}-PL}{PL_{max}-PL_{min}}$	$J_{2,pu} = \frac{VD_{max}-VD}{VD_{max}-VD_{min}}$	$\min(J_{1,pu}, J_{2,pu})$
1	1.0	0.0	4.27644	0.02331	1	0	0
2	0.9	0.1	4.31683	0.01284	0.94982	0.47461	0.47461
3	0.8	0.2	4.40142	0.00569	0.84474	0.79893	0.79893
4	**0.7**	**0.3**	**4.43982**	**0.00411**	**0.79904**	**0.87062**	**0.79904**
5	0.6	0.4	4.49653	0.00269	0.72659	0.93511	0.72659
6	0.5	0.5	4.52067	0.00228	0.69660	0.95364	0.6966
7	0.4	0.6	4.54198	0.00205	0.67013	0.96407	0.67013
8	0.3	0.7	4.57093	0.00184	0.63417	0.97332	0.63417
9	0.2	0.8	4.61642	0.00165	0.57765	0.98226	0.57765
10	0.1	0.9	4.71905	0.00142	0.45016	0.99265	0.45016
11	0.0	1.0	5.08142	0.00126	0	1	0

The bold numbers correspond to the best compromise Pareto optimal solution.

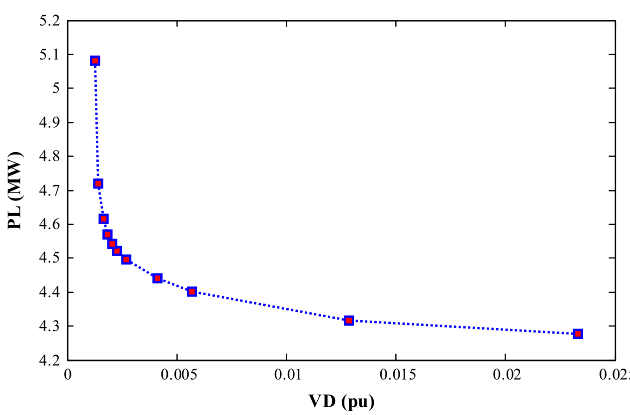

Fig. 6. Pareto front of deterministic case for IEEE 30-bus system.

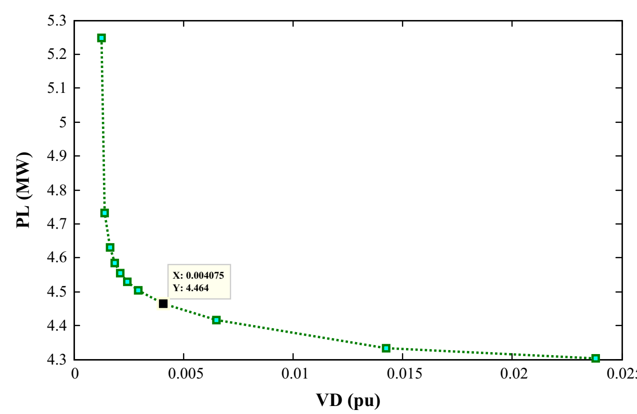

Fig. 7. Pareto front of TPEM for IEEE 30-bus system.

Table 6
Pareto optimal solution of TPEM for IEEE 30-bus system.

#	w_1	w_2	*PL* (MW)	*VD* (pu)	$J_{1,pu} = \frac{PL_{max}-PL}{PL_{max}-PL_{min}}$	$J_{2,pu} = \frac{VD_{max}-VD}{VD_{max}-VD_{min}}$	$\min(J_{1,pu}, J_{2,pu})$
1	1.0	0.0	4.30268	0.02379	1	0	0
2	0.9	0.1	4.33289	0.01425	0.96803	0.42378	0.42378
3	0.8	0.2	4.41618	0.00651	0.87991	0.76750	0.76750
4	**0.7**	**0.3**	**4.46399**	**0.00408**	**0.82932**	**0.87547**	**0.82932**
5	0.6	0.4	4.50329	0.00294	0.78774	0.92578	0.78774
6	0.5	0.5	4.5299	0.00244	0.75959	0.94828	0.75959
7	0.4	0.6	4.55421	0.00213	0.73386	0.96167	0.73386
8	0.3	0.7	4.58568	0.00188	0.70057	0.97295	0.70057
9	0.2	0.8	4.63158	0.00165	0.65201	0.98306	0.65201
10	0.1	0.9	4.73173	0.00141	0.54604	0.99381	0.54604
11	0.0	1.0	5.24781	0.00127	0	1	0

The bold numbers correspond to the best compromise Pareto optimal solution.

Table 7
Pareto optimal solution of MCS for IEEE 30-bus system.

#	w_1	w_2	*PL* (MW)	*VD* (pu)	$J_{1,pu} = \frac{PL_{max}-PL}{PL_{max}-PL_{min}}$	$J_{2,pu} = \frac{VD_{max}-VD}{VD_{max}-VD_{min}}$	$\min(J_{1,pu}, J_{2,pu})$
1	1.0	0.0	4.29858	0.02343	1	0	0
2	0.9	0.1	4.32877	0.01442	0.96781	0.40721	0.40721
3	0.8	0.2	4.41204	0.00661	0.87901	0.76024	0.76024
4	**0.7**	**0.3**	**4.45897**	**0.00421**	**0.82896**	**0.86850**	**0.82896**
5	0.6	0.4	4.49929	0.00301	0.78596	0.92281	0.78596
6	0.5	0.5	4.52747	0.00246	0.75591	0.94768	0.75591
7	0.4	0.6	4.55584	0.00209	0.72565	0.96452	0.72565
8	0.3	0.7	4.58361	0.00187	0.69604	0.97424	0.69604
9	0.2	0.8	4.62892	0.00165	0.64773	0.98444	0.64773
10	0.1	0.9	4.7242	0.00144	0.54612	0.99394	0.54612
11	0.0	1.0	5.23631	0.00130	0	1	0

The bold numbers correspond to the best compromise Pareto optimal solution.

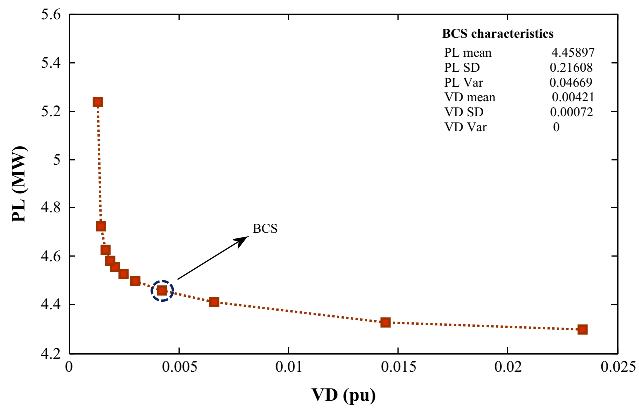

Fig. 8. Pareto front of MCS for IEEE 30-bus system.

Table 8
Control variables for the best solution in IEEE 30-bus system.

Control variables	Deterministic approach	MCS (mean)	TPEM (mean)
Generator variables			
Vg_1 (pu)	1.02287	1.01984	1.01962
Vg_2 (pu)	1.01621	1.01302	1.01296
Vg_5 (pu)	1.00636	1.00347	1.00342
Vg_8 (pu)	0.99956	0.099632	0.99638
Vg_{11} (pu)	1.00577	1.00389	1.00322
Vg_{13} (pu)	1.01696	1.01397	1.01353
Pg_1 (MW)	60.30136	60.8497	60.9537
Shunt compensation ($Q_C \times A$)			
Qc_{10} (MVar)	0	0	0
Qc_{12} (MVar)	0	0	0
Qc_{15} (MVar)	1×6	0.7481×6	1×6
Qc_{17} (MVar)	1×6	0.9484×6	1×6
Qc_{20} (MVar)	0	0.0515×6	0
Qc_{21} (MVar)	1×6	0.9785×6	1×6
Qc_{23} (MVar)	0	0	0
Qc_{24} (MVar)	1×6	0.8756×6	1×6
Qc_{29} (MVar)	0	0.5748×6	0.5×6
Transformer tap changer			
T_{6-9}	0.97062	0.9685	0.96949
T_{6-10}	1.1	1.0998	1.1
T_{4-12}	0.9809	0.9746	0.98136
T_{28-27}	0.99198	0.9947	0.99654

particular, the MATLAB function RANDN provides normally distributed random numbers directly.

In this method, 10,000 random variables are selected for considering the stochastic behavior of the loads. Due to the large number of MCS samples, just some statistical parameters such as mean, standard deviation (SD) and variance (Var) of the answers are presented here. Table 3 shows the mean value of both objective functions for all 11 Pareto optimal solutions. Among these optimal solutions, Solution#7 is the BCS. The Pareto optimal front of the objective functions is derived, which is depicted in Fig. 5. The characteristics of this solution, i.e. its mean and standard deviation for both objectives are also given in this figure.

Control variables in Case I

Table 4 summarizes the obtained control variables for Case I. It is observed that the obtained results by TPEM method is very close to those obtained by MCS, which shows the efficiency of the TPEM method.

Case II: IEEE-30 bus system

Deterministic optimization

Similar to Case-I, the Pareto front is obtained for IEEE 30-bus test system without considering load uncertainty. Table 5 summarizes the information of the Pareto solutions for this case. Fig. 6 shows the Pareto front for Case II. It is evident from the last column of Table 5 that the BCS is Solution#4, with the maximum weakest membership function of 0.79904. The corresponding MO-ORPD problem *PL* and *VD* are equal to 4.43982 MW and 0.00411 pu, respectively.

Uncertainty characterization using TPEM

The load uncertainty is modeled using TPEM for Case II and results of Pareto solutions are presented in Table 6. Fig. 7 shows the Pareto front for Case II with considering load uncertainty using TPEM.

Uncertainty characterization using MCS

The MCS method is used for load uncertainty modeling in this case. Similar to Case I, 10,000 different samples are selected for loads based on the normal distribution. Table 7 summarizes the obtained results using MCS for Case II. Also, the optimal Pareto front is depicted in Fig. 8. It is observed from Table 7 that the BCS is Solution#4 in this case. The characteristics of this solution, i.e. its mean and standard deviation for both objectives are also given in Fig. 8.

Control variables in Case II

Table 8 summarizes the obtained control variables for Case II. Similar to Case I, the results obtained by TPEM approach is close to those obtained by MCS, which means that the TPEM method could be employed to deal with uncertainties in the case of uncertain MO-ORPD problem.

Comparison and discussion

Table 9 compares the obtained results for Case I and Case II with the previously published works. As can be observed from this table, the proposed model can obtain better results compared with the heuristic methods.

Table 9
Comparison of obtained results for deterministic cases with previously published methods.

Case #	Solution	Values							
		PL (MW)				*VD* (pu)			
Case I	Method	Proposed	DE [10]	PSO [10]	ACO [7]	Proposed			
	PL minimization	**13.08294**	13.239	13.25	13.1226	**0.02925**			
	VD minimization	**14.33382**				**0.00147**			
	BCS	**13.29397**				**0.00628**			
Case II	Method	Proposed	DE [43]	QOTLBO [12]	HBMO [22]	Proposed	QOTLBO [12]	HBMO [22]	DE [43]
	PL minimization	**4.27644**	4.555	4.5594	4.40867	**0.02331**	1.9057	0.87364	1.9589
	VD minimization	**5.08142**	6.4755	6.4962	5.20924	**0.00126**	0.0856	0.2106	0.0911
	BCS	**4.43982**		5.2594	5.53522	**0.00411**	0.1210	0.87664	

Table 10
Comparison between the results of TPEM and other methods in Case I (IEEE 14-bus system).

Case I	Deterministic approach	TPEM	MCS
PL (MW)	13.29397	13.30514	13.30991
VD (pu)	0.00628	0.00625	0.006128
Number of run	1	56	10,000
Computing time (min)	0.374	14.862	315.278

Table 11
Comparison between the results of TPEM and other methods in Case II (IEEE 30-bus system).

Case II	Deterministic approach	TPEM	MCS
PL (MW)	4.43982	4.46399	4.45897
VD (pu)	0.00411	0.00408	0.00421
Number of run	1	120	10,000
Computing time (min)	1.399	147.32	1515.02

Tables 10 and 11 compare the obtained objective functions (J_1 and J_2) value for the BCS in TPEM, MCS and deterministic approach for Cases I and II, respectively. On the other hand, because of considering the load uncertainty in the TPEM and MCS, the total expected real power losses in both cases are higher than the deterministic approach. Moreover, it is inferred from these tables that the results obtained by the TPEM and MCS are very close. This means the fact that the TPEM is an accurate method for dealing with such a probabilistic model. However, the number of runs and execution time of TPEM is much less than MCS. Therefore, with a reasonable approximation for both objective functions values, the performance of TPEM is desired in probabilistic MO-ORPD problem.

Conclusions

Multi objective reactive power dispatch (MO-ORPD) problem is studied in this paper considering the load uncertainty. The objective functions used in the proposed probabilistic MO-ORPD problem are real power losses and voltage deviations (from their corresponding nominal values). The stochastic behavior of load is simulated using two-point estimate method (TPEM) and Monte Carlo simulation (MCS). Mixed integer nonlinear programming model is developed for the proposed MO-ORPD problem. The proposed method is implemented and analyzed on two standard test cases, and its effectiveness is verified using different simulations and comparisons. The proposed model yields better results in comparison with previously proposed heuristic algorithms for deterministic cases. Also, the results of case studies show that the obtained values for both objective functions in MO-ORPD using TPEM is very close to the corresponding values obtained by MCS. However, the number of runs and the execution time of TPEM are much less than the MCS. Therefore, in order to save the computation time while maintaining the reasonable approximation for the objective functions value, the TPEM is preferred to deal with the probabilistic MO-ORPD problem.

References

[1] Zehar K, Sayah S. Optimal power flow with environmental constraint using a fast successive linear programming algorithm: application to the algerian power system. Energy Convers Manage 2008;49(11):3362–6.
[2] Shi L, Wang C, Yao L, Ni Y, Bazargan M. Optimal power flow solution incorporating wind power. IEEE Syst J 2012;6:233–41.
[3] Rabiee A, Parniani M. Optimal reactive power dispatch using the concept of dynamic VAR source value. In: Power & energy society general meeting, 2009 PES'09 IEEE. IEEE; 2009. p. 1–5.
[4] Zhao B, Guo C, Cao Y. A multiagent-based particle swarm optimization approach for optimal reactive power dispatch. IEEE Trans Power Syst 2005;20(2):1070–8.
[5] Zhang Y-j, Ren Z. Optimal reactive power dispatch considering costs of adjusting the control devices. IEEE Trans Power Syst 2005;20(3):1349–56.
[6] Khazali A, Kalantar M. Optimal reactive power dispatch based on harmony search algorithm. Int J Electr Power Energy Syst 2011;33:684–92.
[7] Ghasemi M, Ghanbarian MM, Ghavidel S, Rahmani S, Mahboubi Moghaddam E. Modified teaching learning algorithm and double differential evolution algorithm for optimal reactive power dispatch problem: a comparative study. Inform Sci 2014;278:231–49.
[8] Das DB, Patvardhan C. Reactive power dispatch with a hybrid stochastic search technique. Int J Electr Power Energy Syst 2002;24:731–6.
[9] Hu Z, Wang X, Taylor G. Stochastic optimal reactive power dispatch: formulation and solution method. Int J Electr Power Energy Syst 2010;32:615–21.
[10] Varadarajan M, Swarup K. Differential evolutionary algorithm for optimal reactive power dispatch. Int J Electr Power Energy Syst 2008;30:435–41.
[11] Abido M, Bakhashwain J. Optimal VAR dispatch using a multiobjective evolutionary algorithm. Int J Electr Power Energy Syst 2005;27:13–20.
[12] Mandal B, Roy PK. Optimal reactive power dispatch using quasi-oppositional teaching learning based optimization. Int J Electr Power Energy Syst 2013;53:123–34.
[13] Darabian M, Mohseni Bonab SM, Mohammadi-Ivatloo B. Improvement of power system stability by optimal SVC controller design using shuffled frog-leaping algorithm. IETE J Res 2015;61(2):160–9.
[14] Rabiee A, Vanouni M, Parniani M. Optimal reactive power dispatch for improving voltage stability margin using a local voltage stability index. Energy Convers Manage 2012;59:66–73.
[15] Chen G, Liu L, Song P, Du Y. Chaotic improved PSO-based multi-objective optimization for minimization of power losses and L index in power systems. Energy Convers Manage 2014;86:548–60.
[16] Pal BB, Biswas P, Mukhopadhyay A. GA based FGP approach for optimal reactive power dispatch. Proc Technol 2013;10:464–73.
[17] Dai C, Chen W, Zhu Y, Zhang X. Reactive power dispatch considering voltage stability with seeker optimization algorithm. Electr Power Syst Res 2009;79:1462–71.
[18] Jeyadevi S, Baskar S, Babulal C, Willjuice Iruthayarajan M. Solving multiobjective optimal reactive power dispatch using modified NSGA-II. Int J Electr Power Energy Syst 2011;33:219–28.
[19] Saraswat A, Saini A. Multi-objective optimal reactive power dispatch considering voltage stability in power systems using HFMOEA. Eng Appl Artif Intell 2013;26(1):390–404.
[20] Ghasemi M, Ghavidel S, Ghanbarian MM, Habibi A. A new hybrid algorithm for optimal reactive power dispatch problem with discrete and continuous control variables. Appl Soft Comput 2014;22:126–40.
[21] Mallipeddi R, Jeyadevi S, Suganthan PN, Baskar S. Efficient constraint handling for optimal reactive power dispatch problems. Swarm Evol Comput 2012;5:28–36.
[22] Ghasemi A, Valipour K, Tohidi A. Multi objective optimal reactive power dispatch using a new multi objective strategy. Int J Electr Power Energy Syst 2014;57:318–34.
[23] Soroudi A, Rabiee A. Optimal multi-area generation schedule considering renewable resources mix: a real-time approach. IET Gener Transm Distrib 2013;7(9):1011–26.
[24] Mohseni-Bonab SM, Rabiee A, Mohammadi-Ivatloo B. Voltage stability constrained multi-objective optimal reactive power dispatch under load and wind power uncertainties: a stochastic approach. Renew Energy 2016;85:598–609.
[25] Alipour M, Mohammadi-Ivatloo B, Zare K. Stochastic risk-constrained short-term scheduling of industrial cogeneration systems in the presence of demand response programs. Appl Energy 2014;136:393–404.
[26] Rabiee A, Soroudi A, Keane A. Information gap decision theory based OPF with HVDC connected wind farms. IEEE Trans Power Syst 2014.
[27] Kazemi M, Mohammadi-Ivatloo B, Ehsan M. Risk-constrained strategic bidding of GenCos considering demand response. IEEE Trans Power Syst 2014;30(1):376–84.
[28] Soroudi A, Ehsan M. IGDT based robust decision making tool for DNOs in load procurement under severe uncertainty. IEEE Trans Smart Grid 2013;4(2):886–95.
[29] Soroudi A. Robust optimization based self scheduling of hydro-thermal Genco in smart grids. Energy 2013;61:262–71.
[30] Nojavan S, Mohammadi-Ivatloo B, Zare K. Robust optimization based price-taker retailer bidding strategy under pool market price uncertainty. Int J Electr Power Energy Syst 2015;73:955–63.
[31] Soroudi A, Amraee T. Decision making under uncertainty in energy systems: state of the art. Renew Sustain Energy Rev 2013;28:376–84.
[32] Baran ME, Wu FF. Network reconfiguration in distribution systems for loss reduction and load balancing. IEEE Trans Power Deliv 1989;4(2):1401–7.
[33] Ochoa LF, Harrison GP. Minimizing energy losses: optimal accommodation and smart operation of renewable distributed generation. IEEE Trans Power Syst 2011;26(1):198–205.
[34] Mohseni-Bonab SM, Rabiee A, Jalilzadeh S, Mohammadi-Ivatloo B, Nojavan S. Probabilistic multi objective optimal reactive power dispatch considering load uncertainties using Monte Carlo simulations. J Oper Autom Power Eng 2015;3(1):83–93.
[35] Deb K. Multi-objective optimization using evolutionary algorithms. John Wiley & Sons; 2001.
[36] Rabiee A, Soroudi A, Mohammadi-Ivatloo B, Parniani M. Corrective voltage control scheme considering demand response and stochastic wind power. IEEE Trans Power Syst 2014;29:2965–73.

[37] Brooke A, Kendrick D, Meeraus A. GAMS release 2.25: a user's guide. Washington, DC: GAMS Development Corporation; 1996.
[38] Drud AS. CONOPT—a large-scale GRG code. ORSA J Comput 1994;6:207–16.
[39] The GAMS Software Website; 2013. <http://www.gams.com/dd/docs/solvers/sbb.pdf1>.
[40] Morales JM, Perez-Ruiz J. Point estimate schemes to solve the probabilistic power flow. IEEE Trans Power Syst 2007;22(4):1594–601.
[41] Su C-L. Probabilistic load-flow computation using point estimate method. IEEE Trans Power Syst 2005;20(4):1843–51.
[42] Zimmerman RD, Murillo-Sánchez CE, Thomas RJ. MATPOWER: steady-state operations, planning, and analysis tools for power systems research and education. IEEE Trans Power Syst 2011;26:12–9.
[43] El Ela AA, Abido M, Spea S. Differential evolution algorithm for optimal reactive power dispatch. Electr Power Syst Res 2011;81(2):458–64.